Acta Med. Okayama, 2019
Vol. 73, No. 3, pp. 213-221

Acta Medica Okayama
http://escholarship.lib.okayama-u.ac.jp/amo/

Original Article

Spiral Trajectory Modulation of Rheotaxic Motile Human Sperm in Cylindrical Microfluidic Channels of Different Inner Diameters

Saori Nishina[a,b], Koji Matsuura[a,b]*, and Keiji Naruse[a]

[a]*Cardiovascular Physiology, Okayama University Graduate School of Medicine, Dentistry and Pharmaceutical Sciences, Okayama 700-8558, Japan,* [b]*Department of Biomedical Engineering, Faculty of Engineering, Okayama University of Science, Okayama 700-0005, Japan*

We investigated the relationship between human sperm rheotaxis and motile sperm trajectories by using poly-(dimethylsiloxane) (PDMS)-based cylindrical microfluidic channels with inner diameters of 100 μm, 50 μm, and 70 μm, which corresponded to the inner diameter of the human isthmus, the length of a sperm and a diameter intermediate between the two, respectively. We counted the number of rheotaxic sperm and sperm with spiral motion. We also analyzed motile sperm trajectories. As the cylindrical channel diameter was decreased, the percentage of sperm cells exhibiting rheotaxis, the percentage of sperm cells exhibiting spiral motion, the frequency-to-diameter ratio of the sperm cells' spiral trajectories, and the surface area of the microfluidic channel increased, while the flagellar motion at the channel wall decreased. The percentage of sperm exhibiting a spiral trajectory and the frequency-to-diameter ratio of the sperm cells' spiral trajectories were thus affected by the channel diameter. Our findings suggest that the oviduct structure affects the swimming properties of sperm cells, guiding them from the uterus to the ampulla for egg fertilization. These results could contribute to the development of motile sperm-sorting microfluidic devices for assisted reproductive technologies.

Key words: sperm motility, trajectory, microfluidic channel, rheotaxis, oviduct structure

Although 100-300 million human sperm are ejaculated into the vagina during intercourse, few motile human sperm succeed in fertilizing eggs in the ampulla [1]. Peristalsis of the female reproductive tract confers physical stress on sperm, resulting in oxidative damage [2,3]. Sperm must also maintain their ability to fertilize despite obstacles in the female oviduct, and they travel distances >1,000 times their length [4,5]. The isthmus and the ampulla in the oviduct are located in the proximal and distal portions of the uterus, respectively, and the inner diameter of the isthmus is narrower than that of the ampulla [6]. Ejaculated sperm enter the isthmus and undergo capacitation for fertilization in the sperm reservoir at the isthmus [7]. Only when the sperm cells reach the ampulla can some of them fertilize the eggs. Sperm cells use physical and molecular cues to guide their motion on this long and difficult journey.

On the basis of *in vitro* studies of mammalian sperm taxis, three different guidance mechanisms have been proposed: thermotaxis, *i.e.*, swimming in response to a temperature gradient (seen in rabbits and humans) [8]; chemotaxis, which is recognizing a concentration gradient of a chemoattractant and moving to regions of higher concentration (seen in humans [9], rabbits [10],

Received August 27, 2018; accepted February 4, 2019.
*Corresponding author. Phone: +81-86-256-9553; Fax: +81-86-256-9553
E-mail: kmatsuura@bme.ous.ac.jp (K. Matsuura)

Conflict of Interest Disclosures: No potential conflict of interest relevant to this article was reported.

and mice [11]) [1]; and rheotaxis, or sensing mechanical stimuli induced by fluid flow (seen in mice and humans) [12]. Only 3-5% of human sperm show thermotaxis [8], and only 2-12% of human sperm [13, 14] and 10% of mouse sperm [11, 13, 15] show chemotaxis. In mammalian sperm, thermotaxis is driven by the temperature difference between the ampulla and the isthmus. Chemotaxis is a temporary, short-term cue with a range of only a few millimeters, and thus is only effective in guiding the entry of sperm into an egg [1, 13]. In contrast, 80-84% of bull sperm [16] and 49% of human sperm [4] show rheotaxis, which is the principal mechanism underlying the transit of mammalian sperm cells from the vagina to the eggs in the ampulla [12].

We are interested in the relationship between rheotaxis and the linear or spiral swimming trajectories of sperm cells in microfluids, because it is this swimming behavior that guides the sperm to the ampulla. Stable, ascending, and spiral motions of the mammalian sperm cells are induced by the interplay between fluid shear and the chirality of the flagellar beat, and by steric surface-interactions in microfluids [5, 17]. The flagellar motion of sperm cells is perturbed by fluid viscosity, with side-to-side movement more strongly restricted in viscous fluids [18-25]. The linearity of motile sperm increases in microfluidic channels with diameters of 30-50 μm [26]. According to these prior reports, sperm motility is regulated by flagellar motion, fluid mechanical properties, and restricted microfluidic structure. The length of the microfluidic channel for sperm motion is approximately 1-10 mm [26]. Mammalian sperm cells have been observed swimming in bulk buffer but not in narrow microfluidic channels [26, 27].

To accurately investigate sperm motility in restricted spaces, motile sperm should be observed in a channel with an appropriately small diameter. The use of cylindrical microfluidic channels with a diameter similar to the human sperm length (50 μm) and the human isthmus inner diameter (100 μm) enables us to investigate the influence of sperm motion in a restricted space and the effects of a fluid's shear velocity on the spiral trajectory of motile sperm cells.

In this study, we investigated the relationship between motile human sperm rheotaxis and spiral trajectory using poly(dimethylsiloxane) (PDMS)-based cylindrical microfluidic channels with three different inner diameters: 100 μm (which is the approximate inner diameter of the human isthmus), 50 μm (the approximate sperm length), and 70 μm (an intermediate diameter between 50 and 100 μm). We chose PDMS-based microfluidic devices because they offer an easy and efficient way to prepare cylindrical microfluidic channels [28-32]. The PDMS-based cylindrical microfluidic channels of 50-, 70-, and 100-μm diameter were supplied with a continuous flow of water. We analyzed the effects of motile sperm rheotaxis on the spiral trajectories of motile sperm by determining the relationship between rheotaxis and spiral trajectory and the inner diameter of the cylindrical microfluidic channels. Finally, we discuss the implications of our findings in terms of the physiological behavior of motile sperm in the oviducts and the design of improved motile sperm-sorting devices.

Materials and Methods

Microfluidic device design and fabrication. Fig. 1 (A, B) shows the microfluidic device used in this study. The device has a cylindrical microfluidic channel with two different diameters: 500 μm in the lower region and 50, 70, or 100 μm in the higher region (the narrow cylindrical channel) (Fig. 1B). A diluted semen sample was injected into the chosen region with a syringe, and the sperm cell motion in the channel was observed by optical microscopy. The length of the narrow cylindrical channel region was 3-13 mm, as shown in Fig. 1C.

The microchannel was fabricated using PDMS (Momentive Performance Materials Japan, Tokyo). Masters were prepared using a poly(methacrylate) (PMMA) plate (Mitsubishi Chemicals, Tokyo) and a 500-μm hypodermic needle. Narrow microfluidic channels were prepared using 50-μm sutures (Covidien, Dublin, Ireland), 70-μm sutures (Keisei Medical Industrial Co., Tokyo), or 100-μm platinum or tungsten wire (Niraco, Tokyo). The outer frame was made from PMMA. The molds of the microchannel were fabricated by attaching a 500-μm hypodermic needle and other thin suture or wire.

After preparation of the masters, the PDMS monomer and curing agent were mixed in a ratio of 10 : 1 by weight, degassed, and poured into the microchannel mold. The PDMS was cured in an oven (EYELA NDO-400; Tokyo Rikakikai Co., Tokyo) at 70-80°C for > 1.5 h. After curing, the microchannel molds were removed from the channels.

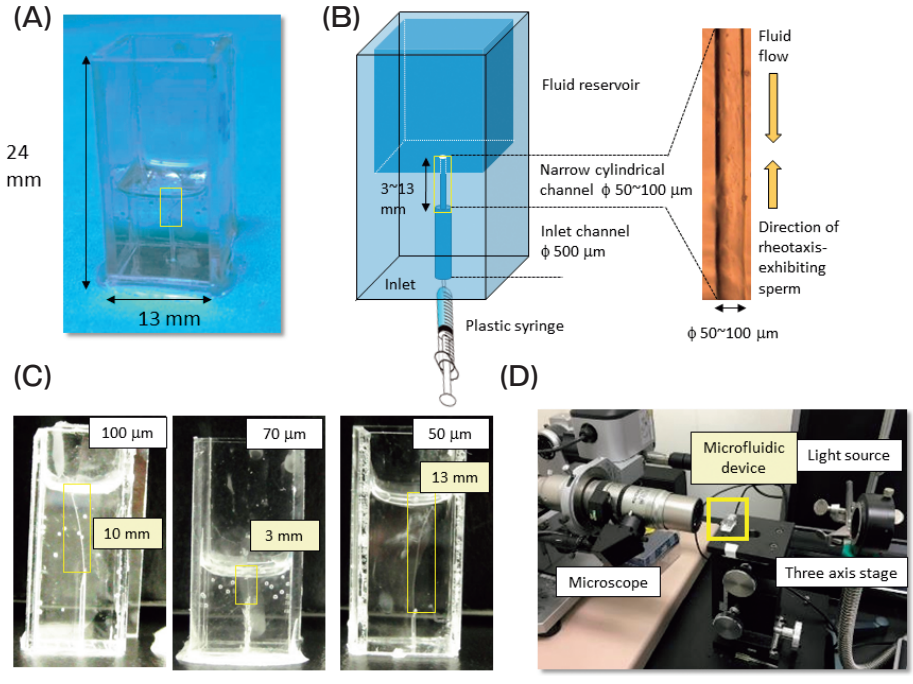

Fig. 1 **A**, The microfluidic device used in this study. The *yellow square* shows the narrow cylindrical channel region of the microfluidic device; **B**, Schematic representation of the microfluidic device and a picture of narrow cylindrical channel region observed by microscopy. Fluid is initially injected from the inlet via a plastic syringe, and it goes to the fluid reservoir. Downward fluid flow is begun by the water head of the fluid in the reservoir; **C**, Photos of the microfluidic devices. The inner diameter and length of the narrow cylindrical channel region are in *white* and *yellow squares*, respectively; **D**, A photo of the observation system.

Table 1 Maximum flow velocity and respective wall shear stress in each narrow cylindrical channel

Diameter of microfluidic channel (μm)	50	70	100
Maximum velocity (μm/sec)	19.8 ± 8.5 (N = 7)	48.6 ± 24.8 (N = 5)	78.0 ± 49.9 (N = 9)
Wall shear stress (mPa*sec)	0.40 ± 0.17	0.69 ± 0.35	0.78 ± 0.50

Construction of the flow gradient system. Human tubal fluid (HTF) (Irvine Scientific, Santa Ana, CA, USA) was injected into the 500-μm diameter inlet channel with a plastic syringe. Diluted semen was then injected in the same way. The fluid flowed by gravity from the upper outlet to the lower inlet of the microfluidic device, and the flow velocity was 6-150 μm/sec. Table 1 shows the maximum flow velocity at the center of the narrow cylindrical channel and the maximum shear stress, which was calculated using the Hagen-Poiseuille flow velocity equation. We used the dispersion of silica particles (1-10 μm diameter) to measure fluid velocity. Small aliquots of silica particles were dispersed in distilled water and injected into the microfluidic channel for observation of the fluid flow. The fluid flow for the sperm rheotaxis experiments was observed using non-motile sperm as tracers.

As noted in Table 1, the observed maximum flow velocities were 19.8 ± 8.5 (n = 7), 48.6 ± 24.8 (n = 5), and 78.0 ± 49.6 (n = 9) μm/sec in the 50-, 70-, and 100-μm diameter cylindrical channels, respectively. The maximum Reynolds number was approximately 0.013 (130 μm/sec maximum fluid velocity, 100-μm diameter), indicating laminar flow. Wall fluid shear stress is proportional to the maximum fluid velocity/cylindrical channel diameter, and was calculated as 0.40 ± 0.17, 0.69 ± 0.35, and 0.78 ± 0.50 (mPa*sec) in the cylindrical channels with 50-, 70-, and 100-μm diameter, respectively. The maximum flow velocity and fluid shear stress decreased with decreasing diameter of the cylindrical

channel.

Semen and sperm samples. Human semen was supplied by one healthy male volunteer. The use of semen samples from one male volunteer (application no.: 30-7) was approved by the Ethics Committee of Okayama University of Science. After ejaculation, samples were immediately incubated at 37°C for 0.5-1 h for liquefying. The semen was washed by centrifugation at 400 *g* and diluted with HTF (Irvine Scientific), and the sperm-containing suspension was diluted to approximately 1.0×10^7 cells/ml to adjust the sperm concentration for the observation of sperm motility and the comparison of sperm counts using the different-diameter cylindrical microfluidic channels. The diluted concentration complied with the World Health Organization (WHO) criteria for fertile sperm concentration (1.5×10^7 cells/ml) [33].

We used seven semen samples obtained from the same volunteer on different days and did not detect significant difference among the semen samples with regard to concentration ($> 1.0 \times 10^7$ cells/ml) and motility (50-80%). All measurements were taken 2-4 times.

Observation of sperm with and without flow. We used an optical microscope (VX-1000; Keyence, Osaka, Japan) to observe and record the sperm motion in the narrow cylindrical microfluidic channels with or without flow. The frame rate of these movies was 15 or 30 frames/sec. The trajectories of the motile sperm were drawn free hand. The movies could not be analyzed using computer-assisted sperm analysis (CASA) programs, because the contrast of the recordings was too low to recognize the sperm heads.

Statistical analysis. The chi-square test was used to determine the differences in the rate of sperm motion between conditions. Student's *t*-test was used to determine differences in the frequency-to-diameter ratio of the sperm cells' spiral trajectories. To account for the use of multiple tests, we used the Bonferroni correction, and *p*-values < 0.016 (0.05/3 = 0.0167) were considered to be statistically significant for pairs of groups from among 3 groups. *P*-values < 0.05 and < 0.016 were considered significant for one pair of 2 groups and for 3 pairs of 3 groups, respectively.

Results

Sperm rheotaxis in the presence of flow. We compared the percentage of human motile sperm showing positive rheotaxis between narrow cylindrical channels with different diameters. Positive rheotactic sperm swim against the downward flow of the fluid. The percentage of positive rheotaxis was calculated from Eq. (1):

$$\text{Positive rheotaxis} = \frac{(\text{Number of motile sperm swimming against flow}) \times 100}{(\text{Total number of motile sperm})} \quad (1)$$

The percentages of positive rheotactic sperm were 84.8% (50-μm diameter; n = 112), 63.8% (70-μm diameter, n = 163), and 63.0% (100-μm diameter; n = 146) (Fig. 2). The percentage of sperm showing positive rheotaxis in the 50-μm-diameter cylindrical channel was significantly larger than those in the 70- and 100-μm-diameter channels ($p < 0.016$). Even though the wall shear stress in the 100-μm diameter channel was twice that of the 50-μm-diameter channel, the percentage of upward-swimming sperm (rheotaxis) was greater in the narrow channel. This result suggests that the swimming direction of sperm is regulated by the channel structure.

Spiral swimming trajectory in the presence of flow. We compared the percentage of rheotactic sperm showing a spiral trajectory between narrow cylindrical channels with different diameters. We observed that motile sperm swimming close to the channel wall appeared periodically in and out of focus of our camera. If the trajectory of the sperm were a planar sinusoidal motion, the motile sperm image would either stay in focus or be out of focus continuously. We thus considered the

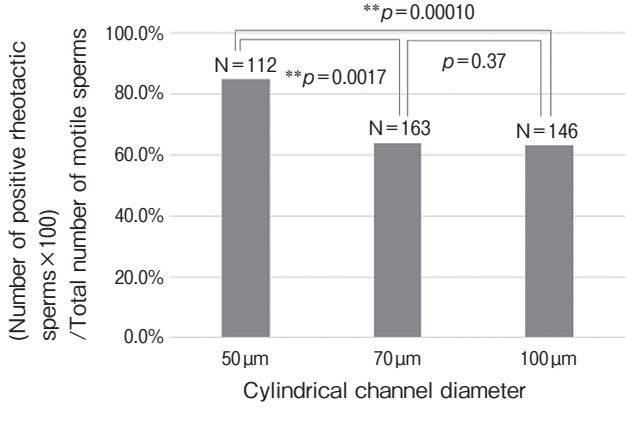

Fig. 2 The percentage of sperm responding to rheotaxis as a function of the narrow cylindrical channel diameter. $^{**}p < 0.016$.

sperm that appeared in and out of focus to exhibit a spiral motion in the narrow cylindrical channel. On the basis of this assay, the percentage of motile sperm exhibiting a spiral trajectory was 41.1% (50-μm diameter, n = 95), 28.8% (70-μm diameter, n = 104), and 16.3% (100-μm diameter, n = 92) (Fig. 3). Thus, more sperm swam spirally in the 50-μm diameter channel than in the 100-μm diameter channel.

Frequency of spiral swimming trajectories in the presence of flow. We visually identified motile sperm heads from our recordings and analyzed their spiral motion. The individual trajectories of the motile sperm cells could be fitted to a sine curve. We calculated the frequency-to-diameter ratio (L/D) of one cycle length (L, the frequency of the sine curve) and the channel diameter (D) (D/2, the amplitude of the sine curve) in the sine curve trajectory as shown in Fig. 4. The L/D ratios (mean ± SD) in the narrow cylindrical channels with 50-, 70-, and 100-μm diameter were 7.8 ± 2.4, 5.8 ± 1.6, and 4.0 ± 1.3, respectively (Fig. 4). Thus, the length of the spiral increased with decreasing cylindrical channel diameter.

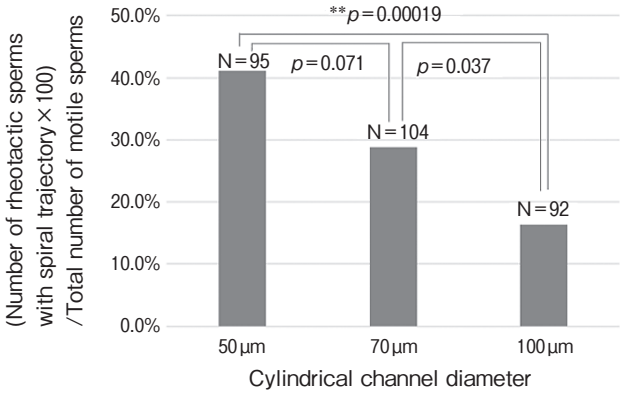

Fig. 3 The percentage of rheotaxis-exhibiting sperm with a spiral trajectory as a function of the narrow cylindrical channel diameter. $^{**}p < 0.016$.

We calculated the angle between the channel direction and the sperm motion based on the L/D. When motile sperm swim spirally with a constant velocity, the angle (θ) can be defined as L/D = 2/tanθ. As the L/D increases (and thus the D decreases), the θ decreases. The calculated θ values in the 50-, 70-, and 100-μm diameter channels were 15°, 19°, and 27°, respectively. Motile sperm with spiral motion can swim more efficiently to their destination in a channel with a smaller diameter.

Percentage of motile sperm showing spiral motion in the presence and absence of flow. Next, we compared the percentages of motile sperm exhibiting spiral motion in the presence and absence of flow (Fig. 5). In the 50-μm diameter channel, the percentage of motile sperm with a spiral trajectory increased from 15% in the absence of flow to 45% in the presence of flow ($p < 0.05$). However, in the 70- and 100-μm diameter channels, the percentage of motile sperm with spiral motion did not greatly increase in the presence of flow. In the 70-μm diameter channel, the percentage of motile sperm showing spiral motion increased from 25% to 28% with flow ($p < 0.05$). In the 100-μm diameter channel, 12% of the sperm were in spiral motion with flow, and 3% of the sperm were in spiral motion without flow; the difference was not significant ($p < 0.05$). The

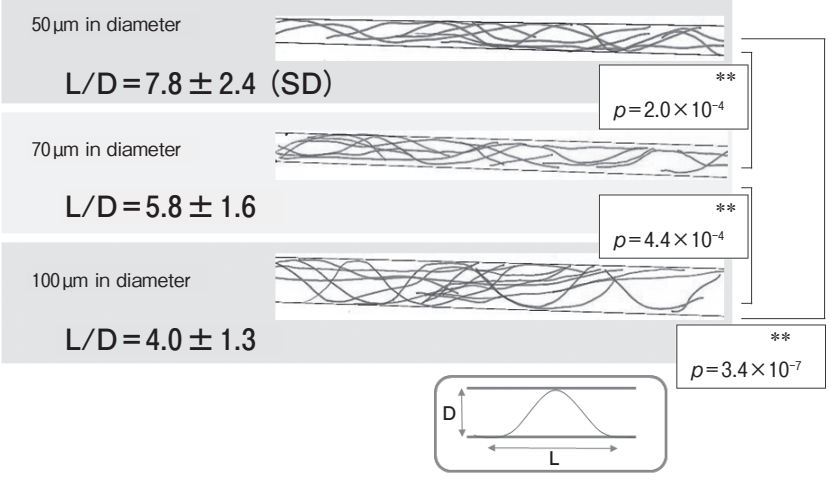

Fig. 4 The trajectory of human sperm under flow. L: The rate of one cycle length for the narrow cylindrical channel diameter (D) (n = 42 for 50 μm, n = 30 for 70 μm, and n = 15 for 100 μm). $^{**}p < 0.016$.

reason for the significant increase in the percentage of motile sperm with spiral motion in the 50-μm diameter cylindrical microfluidic channel is that there was more interaction between the beating flagella and the channel walls compared to the 70- and 100-μm diameter channels. Because many sperm cells swam with linear motion in the 100-μm diameter cylindrical channel without flow, the percentage of sperm with spiral motion decreased in this group. Taken together, our findings revealed that in the narrower microfluidic channel, flow more strongly induced motile sperm cells to swim spirally. This is similar to the result shown in Fig. 3.

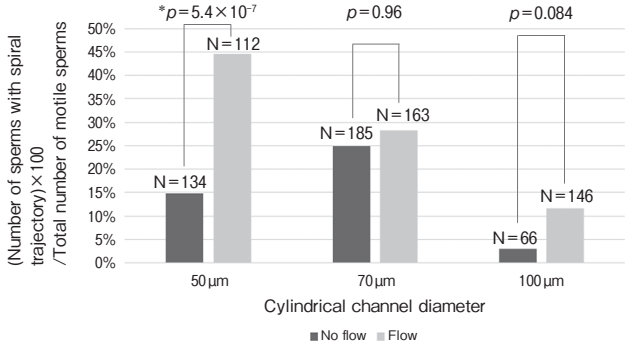

Fig. 5 The percentage of sperm with a spiral trajectory as a function of the narrow cylindrical channel diameter in the presence and absence of fluid flow. $^{*}p < 0.05$.

Discussion

Relationship between motile sperm rheotaxis and the inner diameter of cylindrical microfluidic channels. We compared the percentage of sperm cells exhibiting rheotaxis observed in our experiments with those reported in previous studies (Table 2). As the channel cross-sectional area decreases or the fluid velocity increases, the percentage of sperm cells exhibiting rheotaxis increases due to the increases in the fluid shear rate and stress. El-Sherry *et al*. noted that sperm cells tend to swim near the wall of microfluidic channels with a smaller cross-sectional area under conditions of lower flow velocities [16]. In contrast, our present findings indicate that the shear stress in the 50-μm

Table 2 Comparison of sperm rheotaxis between previous studies and the present investigation

Animal species	Fluid velocity (μm/sec)	Experimental condition or microfluidic channel structure	Rheotaxis (%)	Reference
Bull	33 67 101	Rectangular channel with 50 μm in width and 20 μm in height	68 90 93	16
	33, 67, 101	Rectangular channel with 200 μm in width and 20 μm in height	80–84	
Human	90	Fluid flow from glass micropipette on 35 mm petri dish (Height of fluid, 1,000 μm)	49	4
Human Mouse	10	Fluid flow generated by thermal convection (Width and height of the capillary tube, 1,000 and 50 μm, respectively.)	51 68	12
Human	20	50-μm diameter cylindrical channel	84	This study
	49	70-μm diameter cylindrical channel	63	
	78	100-μm diameter cylindrical channel	63	

diameter channel was half of that in the 100-μm diameter channel. Moreover, the fluid velocity in our study was lower than that used in previous studies [16]. In 2 further studies [4,12], the channel height was greater than that used in our experiment and in the previous study [16], while the shear rate and stress at the wall were lower because of the greater channel height with fluid velocity similar to that used in our experiment [4,12,16].

When we increased the fluid velocity, sperm cells were flushed out of the channel. The rheotactic sperm cell percentage was clearly dependent on the fluid velocity. Rheotaxis was shown to be strongly controlled by the fluid velocity and shear stress distribution in a rectangular channel [16]. We speculate that motile sperm cells with spiral motion tend to swim close to the wall in order to avoid being washed out by carrier fluid motion. The results of our present investigation indicate that rheotaxis is affected by the shear stress and the flow rate of the fluid, and by the dimensions of the channel.

Relationship between the motile sperm spiral trajectory and the inner diameter of cylindrical microfluidic channels. We also compared the spiral motion trajectory that we observed with those reported in previous studies. Miki *et al.* found that spiral motion was induced by fluid flow opposite to the direction of sperm cell motion [12]. We observed a similar phenomenon regarding the induction of sperm cells' spiral motion in cylindrical channels. An important finding of our present study was the relationship between the spiral motion trajectory and the microfluidic channel diameter. Spiral motion of the motile sperm was more frequently observed in the 50-μm diameter cylindrical microfluidic channels (*i.e.*, the channels with diameter similar to the sperm length).

Compared with the flagellar motion in bulk fluid, the flagellar motion of sperm cells in a narrow channel is sterically hindered by the strong interaction of the sperm cells with the wall of the narrow cylindrical channel. The L/D ratio increases as the cylindrical diameter of the microfluidic channel decreases, because the progression of the cells is restricted by their keeping the beating flagella close to the channel wall [5]. Thus, a description of the mechanisms driving the rheotaxis of mammalian sperm cells should include the interaction of flagellar motion with the channel wall.

Effects of motile sperm rheotaxis on their spiral trajectory. We will next discuss regulatory factors and characteristics of sperm flagellar motion in a fluid that affect the trajectory of the sperm cell. The turning behavior of human sperm under flow reversal is dependent on the shear rate and is regulated by changes in the mode of flagellar beating, which switches from rolling and bending to bending only [32]. Sperm motion differs between locations at the channel wall and in bulk fluid because the flagellar beating mode in bulk fluid changes to a slither mode near the surface [22]. Quantitative studies have shown that the side-to-side flagellar movement across the directional axis decreases in high-viscosity medium, and the amplitude of sperm head displacement is dependent on fluid viscosity (the higher the viscosity, the larger the displacement) [19,20].

The micro-scale structure has been shown to influence the trajectory of motile sperm; analogous to our observations of the influence of flagellar motion, ciliary contact with the walls of microfluidic channels has been shown to affect the sperm cell trajectory in *in vitro* studies [25]. In those studies, obstacles or barriers to flagellar motion were shown to increase the linearity of sperm motion. In our present experiments, we observed a difference in sperm trajectories between cylindrical channels with 50- and 100-μm diameters. The amplitude of the side-to-side flagellar movement was restricted by steric hindrance of the channel wall, and thus the angle (θ) of trajectory was smaller than that of the 100-μm diameter channel. We propose that a decrease in the fluid-volume to wall-surface ratio in the channel and an interaction of the sperm flagella with the channel wall serve as cues for sperm directionality and decrease the chance of random motion. Therefore, the motile sperm rheotaxis and spiral motion in a cylindrical microfluidic channel are strongly related. The reason for this is that both sperm behaviors are affected by the flagellar motion perturbation induced by the torque exerted by a vertical flow gradient to the flagella [5].

Comparison of the motile sperm behaviors in cylindrical microfluidic channels and oviducts. The microfluidic channel structure of the isthmus (0.1 mm diameter) guides sperm cells to the ampulla by inducing spiral motion [2,6]. In previous studies, motile sperm cells were channeled to microstructures that mimicked the pockets and crypts in the mucosal folds of the ampulla. Those studies described the microstructure as one of the cues that induced sperm cells to approach the

ampulla. For example, El-Sherry *et al.* reported that positive rheotactic sperm cells showed a tendency to enter circular side pockets (30 μm diameter) along the main microfluidic channel [16]. Taking the previous and present findings together, it seems that when peristaltic oviductal flow in the isthmus is generated, motile sperm cells tend to swim along the luminal surface using spiral motion to migrate toward the ampulla inside the oviduct.

Our present experiments revealed that the sperm cells' trajectory is modulated by the structure of the microfluidic channel and the fluid flow. This suggests that the flagellar motion of the sperm cells is restricted by the channel structure, which alters the frequency of the sperm cells' spiral motion. The development of an experimental system to capture magnified images of motile flagella in a cylindrical channel is necessary to gain a better understanding of the relationship between flagellar motion and microfluidic channel structure. By controlling the channel structure and surface roughness of the microfluidic channel, flagellar beating can be regulated and spiral motion of the sperm cells toward their destination can be induced. The structure of the oviduct is thus physiologically significant for sperm taxis.

Limitations of this study, and further research directions. The limitations of this study and the design of future investigations can be discussed from technical and biological viewpoints. In the present study, we needed a pump and a controller to drive peristaltic flow to mimic the physiological peristaltic movement of the oviduct in an *in vitro* experimental model of sperm motion inside the isthmus. However, it is difficult to observe fluid dynamics inside cylindrical microfluidic channels when using a pump and a controller, as shown in Fig. 1D. The complexity of the system inhibits rapid observation from the side. For observations of three-dimensional sperm spiral motion in the fluid flow, we intend to develop an improved experimental system that includes a computer-based trajectory analysis. With the use of confocal fluorescence microscopy or three-dimensional microscopy, this new system would more clearly recognize motile sperm spiral trajectories and flagellar beating induced by rheotaxis.

Another limitation of this study was the use of only a single volunteer. We need to compare experimental results between sperm samples from healthy persons and patients for examinations of human sperm rheotaxis and the spiral trajectories. The development of a reliable experimental system is necessary for cylindrical microfluidic channel evaluations. Although we currently have the proof-of-concept of this experimental system and a strategy for its further development, we must confirm the proof-of-concept by using sperm samples from several volunteers. The sperm behaviors observed herein arose from the fluid mechanical properties of the motile sperm cells and the microfluid. Therefore, the semen characteristics and genetic backgrounds of healthy persons and patients must be considered when replicating these findings, since differences between these populations would affect the flagellar-beating properties; moreover, the insights obtained could provide clues for identifying male fertility-related markers.

The implications of these insights for the design of improved motile sperm sorting devices for *in vitro* fertilization should be considered. Our results suggest that microfluidic channels with inner diameters < 100 μm can guide motile sperm with spiral motion in the desired direction. The use of an array of microfluidic channels with diameters of 50-100 μm and adequate flow inside the narrow cylindrical channel could improve the motile sperm recovery rate by using these sperm-guiding effects. We intend to develop an experimental system equipped with an array of microfluidic channels in order to increase the concentration of sorted motile sperm. In this way, the efficiency of devices for motile sperm collection could be increased to improve assisted reproductive technologies [29, 34, 35].

In conclusion, we analyzed the relationship between human sperm rheotaxis and motile sperm trajectories in 50-, 70-, and 100-μm diameter cylindrical microfluidic channels with and without fluid flow. We found that the spiral motion of human sperm was modulated by the fluid flow and the microfluidic channel diameter. The percentage of sperm exhibiting spiral motion and the frequency-to-diameter ratio of the spiral trajectory increased in the narrower cylindrical channel (50 μm). As the cylindrical channel diameter decreases, the surface area of the fluid increases, and the sperm flagellar beating would interact with the wall. Both the rheotaxis and the spiral motion of motile sperm were modulated by fluid shear stress distribution in the fluid. We thus conclude that the channel structure affects the sperm

cells' swimming properties and guides them to the ampulla for egg fertilization.

Acknowledgments. This study was supported by grants-in-aid for Scientific Research for Fundamental Sciences (Nos. 26350106 and 18K12069 to K.M., and No. 26220203 to K.N.) from the Ministry of Education, Culture, Sports, Science and Technology (MEXT) of Japan. We thank Enago for the English language review.

References

1. Perez-Cerezales S, Boryshpolets S and Eisenbach M: Behavioral mechanisms of mammalian sperm guidance. Asian J Androl (2015) 17: 628–632.
2. Suarez SS and Pacey AA: Sperm transport in the female reproductive tract. Hum. Reprod. Update (2006) 12: 23–37.
3. Menge AC and Edwards RP: Immunology of reproduction; CRC Press, Boca Raton, FL, USA, (1993) pp.19.
4. Zhang Z, Liu J, Meriano J, Ru C, Xie S, Luo J and Sun Y: Human sperm rheotaxis: a passive physical process. Sci Rep (2016) 6: 23553.
5. Kantsler V, Dunkel J, Blayney M and Goldstein RE: Rheotaxis facilitates upstream navigation of mammalian sperm cells. eLife (2014) 3: 02403.
6. Lyons RA, Saridogan E and Djahanbakhch O: The reproductive significance of human Fallopian tube cilia. Hum Reprod Update (2006) 12: 363–372.
7. Ishikawa Y, Usui T, Yamashita M, Kanemori Y and Baba T: Surfing and swimming of ejaculated sperm in the mouse oviduct. Biol Reprod (2016) 94: 89.
8. Bahat A, Tur-Kaspa I, Gakamsky A, Giojalas LC, Breitbart H and Eisenbach M: Thermotaxis of mammalian sperms cells: a potential navigation mechanism in the female genical tract. Nat Med (2003) 9: 149–150.
9. Ralt D, Manor M, Cohen-Dayag A, Tur-Kaspa I, Ben-Shlomo I, Makler A, Yuli I, Dor J, Blumberg S, Mashiach S and Eisenbach M: Chemotaxis and chemokinesis of human spermsatozoa to follicular factors. Biol Reprod (1994) 50: 774–785.
10. Giojalas LC, Fabro G, Eisenbach M and Rovasio RA: Capacitated and chemotactic rabbit spermsatozoa appear to be shortly available around ovulation. J Androl (2001) 22: 92.
11. Oliveira RG, Tomasi L, Rovasio RA and Giojalas LC: Increased velocity and induction of chemotactic response in mouse spermsatozoa by follicular and oviductal fluids. J Reprod Fertil (1999) 115: 23–27.
12. Miki K and Clapham DE: Rheotaxis guides mammalian sperms. Curr Biol (2013) 23: 443–452.
13. Eisenbach M: Mammalian sperms chemotaxis and its association with capacitaion. Dev Gent (1999) 25: 87–94.
14. Cohen-Dayag A, Ralt D, Tur-Kaspa I, Manor M, Makler A, Dor J, Mashiach S and Eisenbach M: Sequential acquisition of chemotactic responsiveness by human spermsatozoa. Biol Reprod (1994) 50: 786.
15. Giojalas LC and Rovasio R: Mouse spermatozoa modify their motility parameters and chemotactic response to factors from the oocyte microenvironment. Int J Androl (1998) 21: 201–206.
16. El-Sherry TM, Elsayed M, Abdelhafezc HK and Abdelgawad M: Characterization of rheotaxis of bull sperms using microfluidics. Integr Biol (2014) 6: 1111–1121.
17. Ishimoto K and Gaffney EA: Fluid flow and sperm guidance: a simulation study of hydrodynamic sperm rheotaxis. J R Soc Interface (2015) 12: 20150172.
18. Marcos, Tran NP, Saini AR, Ong KCH and Chia WJ: Analysis of a swimming sperm in a shear flow. Microfluid Nanofluid (2014) 17: 809–819.
19. Kirkman-Brown JC and Smith DJ: Sperm motility: is viscosity fundamental to progress? Mol Hum Reprod (2011) 17: 539–544.
20. Smith DJ, Gaffney EA, Gadhêla H, Kapur N and Kirkman-Brown: Bend propagation in the flagella of migrating human sperm, and its modulation by viscosity. J Cell Motil Cytoskelet (2009) 66: 220–236.
21. Ishimoto K, Ikawa M and Okabe M: The mechanics clarifying counterclockwise rotation in most IVF eggs in mice. Sci Rep (2017) 7: 43456.
22. Nosrati R, Driouchi A, Yip CM and Sinton D: Two-dimensional slither swimming of sperm within a micrometre of a surface. Nat Commun (2015) 6: 8703.
23. Nosrati R, Graham PJ, Liu Q and Sinton D: Predominance of sperm motion in corners. Sci Rep (2016) 6: 26669.
24. Guidobaldi A, Jeyaram Y, Berdakin I, Moshchalkov VV, Condat CA, Marconi VI, Giojalas L and Silhanek AV: Geometrical guidance and trapping transition of human sperm cells. Phys Rev (2014) 89: 032720.
25. Denissenko P, Kantsler V Smith DJ and Kirkman-Brown J: Human spermatozoa migration in microchannels reveals boundary-following navigation. Proc Natl Acad Sci (2012) 109: 8007–8010.
26. Magdanz V, Koch B, Sanchez S and Schmidt OG: Sperm Dynamics in Tubular Confinement. Small (2015) 11: 781–785.
27. Khandurina J, McKnight TE, Jacobson SC, Waters LC, Foote RS and Ramsey JM: Integrated system for rapid PCR-based DNA analysis in microfluidic devices. Anal Chem (2000) 72: 2995–3000.
28. Gómez-Sjöberg R, Leyrat AA, Prione DM, Chen CS and Quake SR: Versatile, fully automated, microfluidic cell culture system. Anal Chem (2007) 79: 8557–8563.
29. Ziaiea B, Baldi A, Lei M, Gu Y and Siegel RA: Hard and soft micromachining for BioMEMS: review of techniques and examples of applications in microfluidics and drug delivery. Adv Drug Deliver Rev (2004) 56: 145–172.
30. Chen CY, Tu TY, Chen CH, Jong DS and Wo AM: Patch clamping on plane glass - fabrication of hourglass aperture and high-yield ion channel recording. Lab Chip (2009) 9: 2370–2380.
31. Cho BS, Schuster TG, Zhu X, Chang D, Smith GD and Takayama S: Passively driven integrated microfluidic system for separation of motile sperm. Anal Chem (2003) 75: 1671–1675.
32. Bukatin A, Kukhtevich I, Stoopd N, Dunkel J and Kantslere V: Bimodal rheotactic behavior reflects flagellar beat asymmetry in human sperm cells. Proc Natl Acad Sci (2015) 112: 15904–15909.
33. Cooper TG, Noonan E, Eckardstein S, Auger J, Baker HWG, Behre HM, Haugen TB, Kruger T, Wang C, Mbizvo MT and Vogelsong KM: World Health Organization reference values for human semen characteristics, Hum Reprod Update (2010) 16: 231–245.
34. Matsuura K, Takenami M, Kuroda Y, Hyakutake T, Yanase S and Naruse K: Screening of sperm velocity by fluid mechanical characteristics of a cyclo-olefin polymer microfluidic sperm-sorting device. Reprod Biomed Online (2012) 24: 109–115.
35. Shirota K, Yotsumoto F, Itoh H, Obama H, Hidaka N, Nakajima K and Miyamoto S: Separation efficiency of a microfluidic sperm sorter to minimize sperm DNA damage. Fertil Steril (2016) 105: 315–321.